Ecological Indicators 147 (2023) 110009

Contents lists available at ScienceDirect

Ecological Indicators

journal homepage: www.elsevier.com/locate/ecolind

Original Articles

Exploring the response of ecosystem service value to land use changes under multiple scenarios coupling a mixed-cell cellular automata model and system dynamics model in Xi'an, China

Ping Zhang [a,b,c,d,e,*], Lei Liu [a], Lianwei Yang [a], Juan Zhao [a], Yangyang Li [a], Yuting Qi [a], Xuenan Ma [a], Lei Cao [a]

[a] School of Environmental and Chemical Engineering, Xi'an Polytechnic University, Xi'an 710048, China
[b] State Key Laboratory of Urban and Regional Ecology, Research Center for Eco-Environmental Sciences, Chinese Academy of Sciences, Beijing 100085, China
[c] Shaanxi Key Laboratory of Land Consolidation, Xi'an 710075, China
[d] State Key Laboratory of Green Building in Western China, Xi'an University of Architecture & Technology, Xi'an 710055, China
[e] Xi'an Key Laboratory of Territorial Spatial Information, Xi'an 710075, China

ARTICLE INFO

Keywords:
Ecosystem service value
MCCA
SD
Scenario prediction
Sensitivity analysis

ABSTRACT

Land use is a crucial factor affecting ecosystem service value (ESV), and forecasting future land use changes and ESV response can guide urban planning and sustainable development decisions. However, the traditional Cellular Automata (CA) model supposes that each cell has only one land use type at each time step, neglects the mixed structure and proportional distribution of land use units, does not take into account its quantitative continuous dynamic change, and lacks the exploration of land use quantity structure and spatial pattern optimization. This study employed a novel mixed-cell cellular automata (MCCA) approach, coupled with the system dynamics (SD) model to predict the spatiotemporal pattern of land use under the natural increase scenario (NIS), economic development scenario (EDS) and ecological protection scenario (EPS) in Xi'an, China, in 2030. The equivalent coefficient method was utilized to investigate the heterogeneity distribution and sensitivity of ESV. The results demonstrated that SD-MCCA exhibited remarkable prediction accuracy and robustness. The main changes in land use in 2000–2015 were due to urban expansion, the conversion of arable land into construction land, and the conversion between grassland and arable land. The total ESV increased from 19554.36×10^6 CNY in 2000 to 19618.39×10^6 CNY under the EPS in 2030, and the contribution of climate regulation and hydrological regulation to ESV was the highest. Spatial heterogeneity of ESV revealed a certain regularity, and the high value region was chiefly concentrated in woodland and grassland with favorable ecological conditions. Land use variations under NIS and EPS improved ESV, while the ESV had a negative response to land use transformations under the EDS. This research provides a new way to identify the relationship between future land utilization scenarios and ESV, which is of great significance for the management of land resources and formulation of ecological compensation standards.

1. Introduction

Ecosystem service (ES) refers to the benefits that human beings obtain directly or indirectly from the structure, process and function of ecosystems, mainly includes provisioning, cultural, regulating and supporting services (Costanza et al., 1997; de Groot et al., 2010; Zhang et al., 2020). Monetary assessment of ecosystem service value (ESV) can effectively quantify the benefits that humans derive from the ecosystem, improve people's understanding of the value of natural assets, help decision makers carry out reasonable ecological environment planning, promote regional scientific development and protect ecosystems with high ESVs (Bateman et al., 2013; Fisher et al., 2009; Pueffel et al., 2018). However, with the acceleration of economic development, population growth and urban sprawl, human activities have led to ecosystem degradation, biodiversity reduction and water quality deterioration, further contributing to significant decreases in ESVs (Collin and Melloul, 2001). Land utilization variation is a key index that reflects anthropogenic disturbance to the ecosystem and has significant role in supporting

* Corresponding author.
E-mail address: pingzhang_2008@126.com (P. Zhang).

https://doi.org/10.1016/j.ecolind.2023.110009
Received 21 August 2022; Received in revised form 6 February 2023; Accepted 8 February 2023
Available online 13 February 2023

ES functions. Nevertheless, human overexploitation of land resources has resulted in serious damage to regional ecosystems (Keller et al., 1991). Therefore, exploring the relationship between ESV and land use variations is extremely important for maintaining ecosystem health and the sustainable utilization of land resources (Aziz, 2021; Mendoza-Gonzalez et al., 2012).

In recent years, the response of ESV to land utilization change has attracted increasing attention from researchers in China and abroad (Arowolo et al., 2018; Chen et al., 2021a; Liu et al., 2021b). In southern Sinaola, Mexico, researchers applied remote sensing technology to assess the impact of land use transformation on wetland ESV from 2000 to 2010 (Camacho-Valdez et al., 2014). Kindu et al. (2016) revealed influence of land use dynamics on ESV in Ethiopian highlands from 1973 to 2012 and investigated the contribution differences of different ecosystem service functions. Some researchers have examined the response of ESV in the Pearl River Delta of China to land use transformation through multisource data and detected hot and cold spots (Hu et al., 2019). Dai et al. (2021) verified the distribution features of land utilization and ESV in Chengdu, China, utilized remote sensing images from 2003 to 2018, and further discussed the driving factors of ESV. Akhtar et al. (2022) assessed the spatial-temporal heterogeneity of ESV in dryland ecosystems of Pakistan by combining land use data and GIS analysis techniques and evaluated the causes of ESV reduction. However, previous studies mostly employed historical land use for ESV estimation, and there is still room for investigation into the potential future trend of ESV. The prediction of future land use scenarios and ESV responses can offer a scientific reference for government land planning decisions and ecosystem protection (Peng et al., 2021; Schirpke et al., 2020; Zhang et al., 2015).

Land use models are often applied to forecast the spatiotemporal distribution of ESV with land use conversions (Liu et al., 2021a; Qin and Fu, 2020; Zhang et al., 2019). Das et al. (Das et al., 2021) adopted machine learning and the cellular automata (CA)-Markov model to predict the spatial allocation of ESV in Asian megacities from 2030 to 2050 and clarified the spatial aggregation pattern of ESV. Wu et al. (2020) coupled a linear optimizing technique and the conversion of land use and its effects at a small regional extent (CLUE-S) and assessed the response of ESV to land utilization planning scenarios in 2025. Liu et al. (2020) employed the future land use simulation (FLUS) model to reveal the dynamic evolution of ESV under the scenarios of natural growth, economic growth and ecological conservation in the Bohai Rim coastal region. These researchers integrated multipurpose optimal method and the patch-generating land-use simulation (PLUS) model to evaluate temporal and spatial alterations of ESV in ecological shelter zone in China in 2026 (Li et al., 2021). However, these conventional models hypothesize that every cell is pure and discrete (Pontius et al., 2007). In reality, each cell consists of a mixture of various land utilization types. The mixed-cell cellular automata (MCCA) model can simulate the proportional distribution of mixed land utilization patterns in cells, excavate land use development probability using the random forest (RF) algorithm, and simulate the land use competition mechanism based on multiple roulettes. It can realize the mutual transformation of various land utilization structures at subcellular level and has a higher precision in land application simulation (Liang et al., 2021). Therefore, MCCA approach is a new and effective approach for the multi-scenario modeling of land utilization and future forecasting of ESV.

The combination of land use spatial prediction and quantitative structure simulation model can reveal the spatiotemporal characteristics and internal mechanism of land utilization change, and can more accurately simulate the spatial distribution of land application and ESV (Wang et al., 2022b). Wang et al. (2022a) combined multi-criteria evaluation (MCE) and CA model to predict the spatial and temporal changes of land utilization in Wuhan metropolitan area. Li et al. (2019) integrated Markov and CA to demonstrated the influence of land utilization alterations on ESV in Central Asia from 2025 to 2035. Wang et al. (2018b) established three various of land use scenarios using the multi-objective programming (MOP) and CLUE-S model, and investigated the response law of ESV in Wuhan in 2040. However, the nonlinear influence of socio-economic factors on the quantitative structure of land application has been neglected, and the optimization of the quantitative structure of land utilization has not been considered. SD model can solve the internal feedback between the structure, function and behavior of land utilization, gain the dynamic quantitative information of the system (Letourneau et al., 2012; Zheng et al., 2012), and illuminate the nonlinear correlation mechanism between the socio-economic system and land application in accordance with the construction table function (van Delden et al., 2010), achieve the quantitative structure prediction of land utilization types under varying scenarios in the future. Combining the macro area demand forecast of SD with the micro spatial modeling of MCCA can give full play to the complementary advantages of the coupling model SD-MCCA and enhance the precision of the simulation results of ESV and land application spatial-temporal pattern (Rasmussen et al., 2012; Wu et al., 2022).

The approaches for evaluating ESV are divided into two types: the price each unit ES function and the equivalent coefficient technique in accordance with land use value each unit area (Fu et al., 2022). The previous approach utilizes ecological process models to quantify ESV with comprehensive considerations (Elmqvist et al., 2015). However, it requires too much input data, and the simulation process is too complex, which requires multiple models to participate in the evaluation. It is difficult to unify the standards, which raises the difficulty of its employment and restricts its utilization in research (Liu et al., 2021b; Long et al., 2022). In contrast, the latter method has the advantages of simple operation, a lower data requirement intuitiveness and efficiency and is widely applied in the simulation and prediction of ESV (Bateman et al., 2013; Xing et al., 2021), which can provide support for the calculation of ESV and aid in scientific decision-making.

Xi'an is the core area of the Xi'an Metropolitan Region and the key zone of the Guanzhong Plain urban agglomeration (GPUA), as well as a significant central city in western region of China. It is in a period of accelerated industrialization and urbanization and inevitably faces a variety of ecological and environmental problems (Zhang et al., 2021). Therefore, the coordinated development of its regional ecological economy has important theoretical significance and practical value for the rational allocation of land resources and the sustainable management of its ecosystems. In summary, the purposes of this research are as follows: (1) to validate the simulation accuracy of the MCCA model by combining the land use and driving forces from 2000 to 2015, integrate socio-economic, population change and land use variables to establish SD model, and the quantitative structure and spatial pattern prediction optimization model SD-MCCA was coupled to predict the land use spatial pattern in Xi'an in 2030 under the NIS, EDS and EPS scenarios; (2) to reveal the temporal and spatial variation characteristics of ESV by employing the equivalent coefficient method; and (3) to evaluate the response of ESV to land utilization transformation by applying the sensitivity index. This study provides new insights into the optimization of land utilization quantity structure and pattern layout, and offers policy recommendations for sustainable land resource planning, natural resource protection and ecosystem management.

2. Study area

Xi'an (33°42′-34°45′ N, 107°40′-109°49′ E) is located in the Guanzhong Basin of the Yellow River (Fig. 1). It is the political, cultural and economic core of Shaanxi Province, which has 13 districts and counties, with an area of approximately 10108 km^2. Xi'an has the highest altitude difference among all Chinese cities, and the Qinling Mountains and the Weihe Basin constitute its main landforms. The area has a warm temperate semi humid continental monsoon climate, with an annual mean temperature of 13.1–14.3 ℃. January is the coldest month, and July is the hottest. The annual precipitation is 528.3–716.5 mm. Obvious precipitation peaks occur in July and September, and the

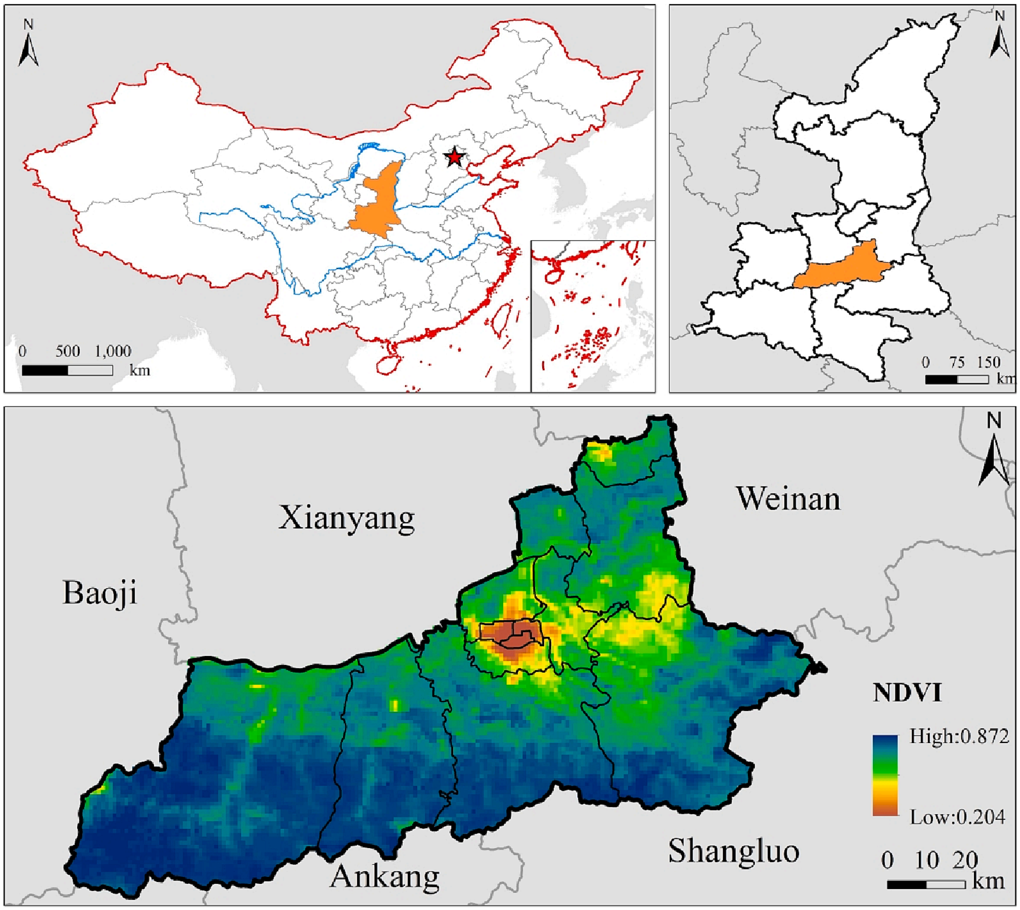

Fig. 1. Location of the Xi'an.

climate changes significantly in the four seasons. It is the largest key metropolis in Northwest China. In February 2018, the Chinese government released the GPUA expansion program, which clearly supports Xi'an in building a national pivotal metropolis and an internationalized city with historical and cultural characteristics.

3. Materials and methods

In this research, we coupled a new mixed land use structure MCCA model and system dynamics SD model to investigate the optimization approach of land utilization quantitative structure and spatial pattern, predict the spatiotemporal evolution rule of land application in the future, and reveal the response mechanism of ESV under multiple scenarios. The framework included the following three steps (Fig. 2): (1) Database establishment. In accordance with the requirements of SD-MCCA model, the acquired data is preprocessed, and the historical land utilization data is transformed into mixed cell data. The driving factors are extracted, interpolated and resampled to the same boundary and resolution. (2) Model coupling. The past land application mixed cell data and driving forces are employed to forecast the conversion matrix and development probability data set, simulate the land utilization alteration in 2015, and verify the precision of the SD-MCCA model. According to population variation, socio-economic and policy orientation, the area and space pattern of various land application types under different scenarios in 2030 are predicted. (3) Future ESV prediction. The value table of ecosystem services per unit area was built by applying the yield and value coefficient of primary grain crops. The spatiotemporal distribution of ESV under various scenarios was evaluated on the basis of the equivalent coefficient method. The sensitivity index was applied to demonstrate the impact of land application transformation on ESV, which provided reference for sustainable development and scientific management of ecosystem services in Xi'an.

3.1. Data sources and treatment

The Resource and Environmental Science Data Center of the Chinese Academy of Sciences provides land utilization and administrative boundaries in 2000 and 2015, the data accuracy is 30 m, in which land use include cultivated land, woodland, grassland, water area, built-up area and bare land. It also offers NDVI, social and economic indicators, and the data precision is 1000 m. The digital elevation model (DEM) with accuracy of 30 m is obtained through the geospatial data cloud platform, from which slope and aspect data were extracted. The Harmonized World Soil Database (HWSD) provided soil data, meteorological data retrieved from the China Meteorological Data Network, containing precipitation and temperature. The distance to the way and administrative center were calculated in ArcGIS (European distance). The earth night light "flint" data set provided night light data at a resolution of 1500 m. Statistical data of Xi'an provided the area and yield of crops. Xi'an Statistical Yearbook and General Land Use Planning from 1978 to 2015 were collected to provide the socio-economic and demographic for the SD model. The raster data used in the study were resampled to the same resolution.

3.2. MCCA model

To predict future multi-scenario changes in land use, a novel mixed cell MCCA model was adopted (Liang et al., 2021). This is a new CA model founded on quantitative conversion rule mining of land use types, land use structure simulation and accuracy evaluation, which is

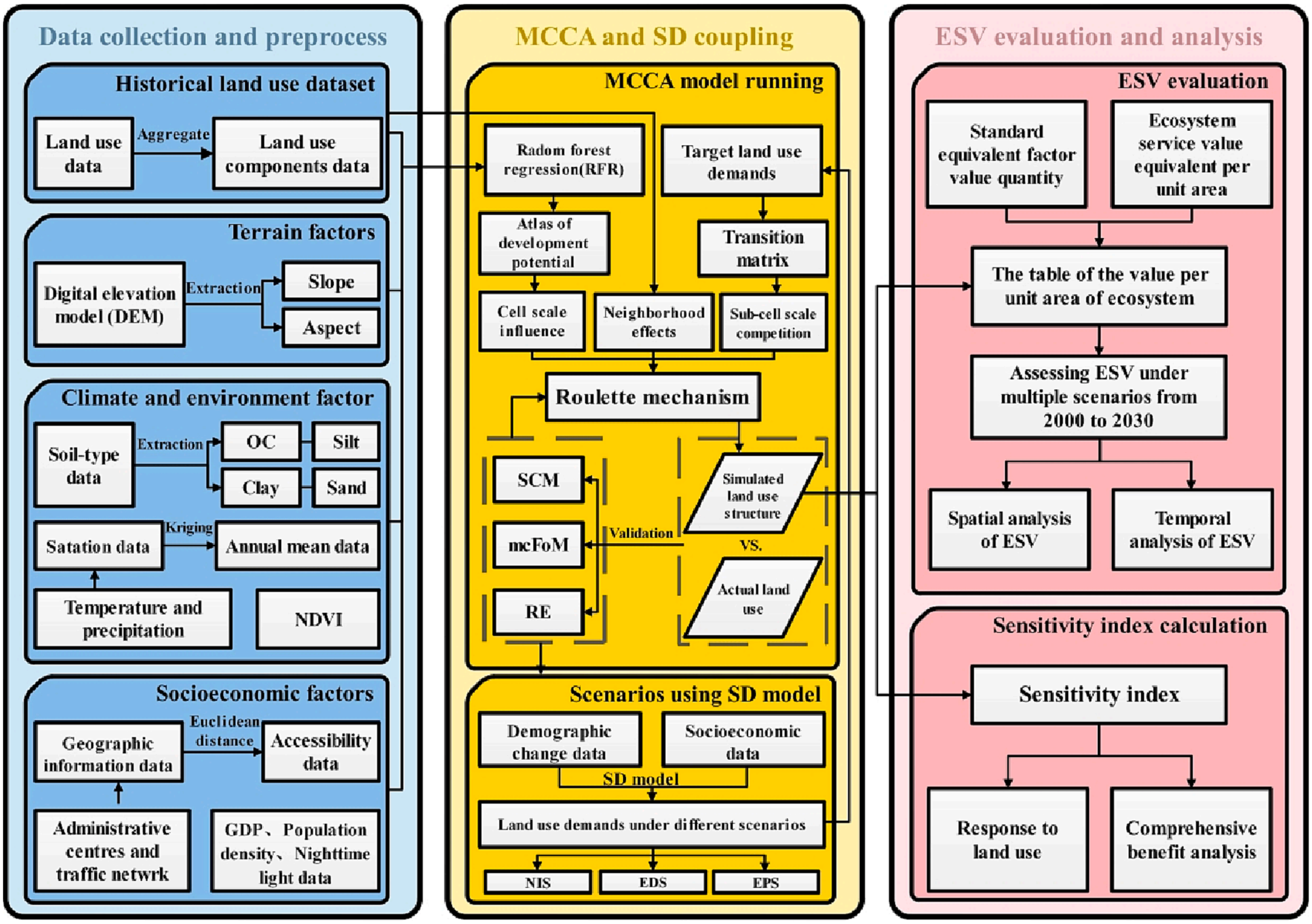

Fig. 2. Flow chart of land utilization prediction and ESV evaluation.

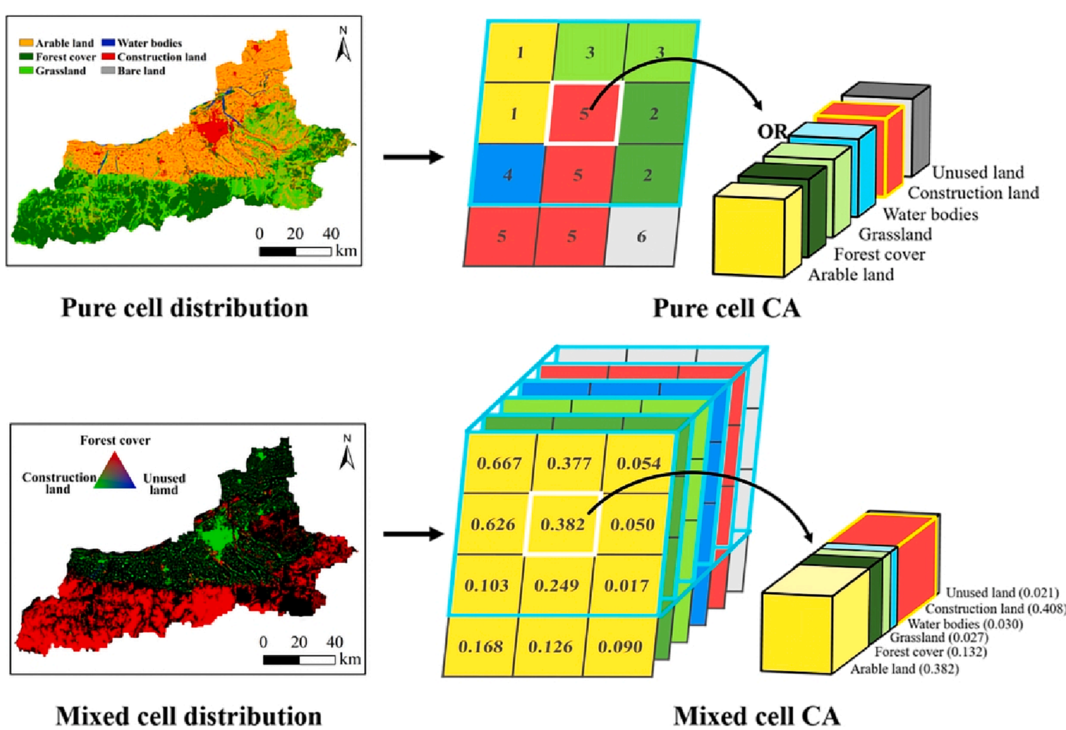

Fig. 3. Difference between pure-cell CA and mixed-cell CA in simulating land use structure.

employed to reveal diversity of land utilization structure and describe land use structure variation more accurately (Fig. 3). Quantitative conversion rule mining of land utilization patterns is utilized to confirm the impact of driving factors on different land utilization composition and obtain the evolution probability. The driving forces were selected from two aspects of natural and social factors. Considering the interaction between pixels and the internal information of pixels, the adaptive chance of different land utilization components was calculated by using random forest algorithm. The modeling of land utilization structure by using MCCA's pixel state, which is composed of a series of components and their interaction relationships within the pixel. We applied roulette wheel to confirm whether the land utilization transformation reaches the expected goal to meet the macro land use demand and micro land application competition. The feedback between land utilization requests and configurations is used to finally achieve the predicted target. The traditional simulation accuracy assessment method is only suitable for the pure CA model, it is difficult to evaluate consecutive and many dimensions indicators. Therefore, a scheme for MCCA accuracy estimation is designed, which includes three parts: (1) RF is exploited to excavate the conversion relation between land utilization structures and impact indicators; (2) structural changes are quantitatively simulated according to transition rules; and (3) the modeling precision is evaluated according to three accuracy indexes (OA, mcFoM and average RE).

3.3. The SD model

The SD model can reflect the interaction between the functions and dynamic behaviors of the components in the nonlinear dynamic variations of the complex system structure with multiple feedbacks. Its advantage lies in the simplification and abstraction of the actual system structure to adapt to diverse policy scenarios and propose corresponding solutions (Huang et al., 2022), a feedback loop is formed during the operation of the model to effectively investigate the dynamic evolution mechanism behind the system. According to the statistical yearbook and general land utilization planning of Xi'an from 1978 to 2015, the data of social economy, population alteration and land application were obtained. The SD model (Fig. 4) was established by using Vensim software. The model simulation period was 2000–2030, and the time step was 1 year. The simulation process was divided into two steps (Wang et al., 2022b). The first step is to utilize the collected historical data to examine the model. By modifying the parameter settings, compare the modeling results with the actual situation to ensure that the constructed model has sufficient precision to simulate the land utilization require in the future with multiple scenarios. The corresponding time period is 2000–2015. The second step is to take into account human activities, policy trends and scenario demands at the same time, regulate the system parameters to acquire the land application requirements under various future scenarios for the next land utilization model simulation, and the corresponding time period is 2015–2030.

3.4. Future scenario setting

To reveal different patterns of urban development in the future, we set three alternative scenarios founded on SD model, namely NIS, EDS and EPS, according to the overall land use planning in Xi'an and with reference to the land use, ecological environment and economic growth of the study area.

The NIS was a benchmark scenario, and the urban future development pattern was consistent with the historical land use variation trend under this scenario. According to the land utilization data, socio-economic and demographic change factors from 2000 to 2015, the SD model is applied to calculate the required area of each land utilization type in 2030. The EDS prioritizes rapid economic development, the population growth rate increased by 10 %, the proportion of urban residents increased by 14 %, the grain yield per unit area increased by 2 % year by year, and the output of construction industry was the highest under three scenarios. The EPS prioritizes ecological benefits; it focuses on protecting land, such as forest cover, grassland and water bodies with

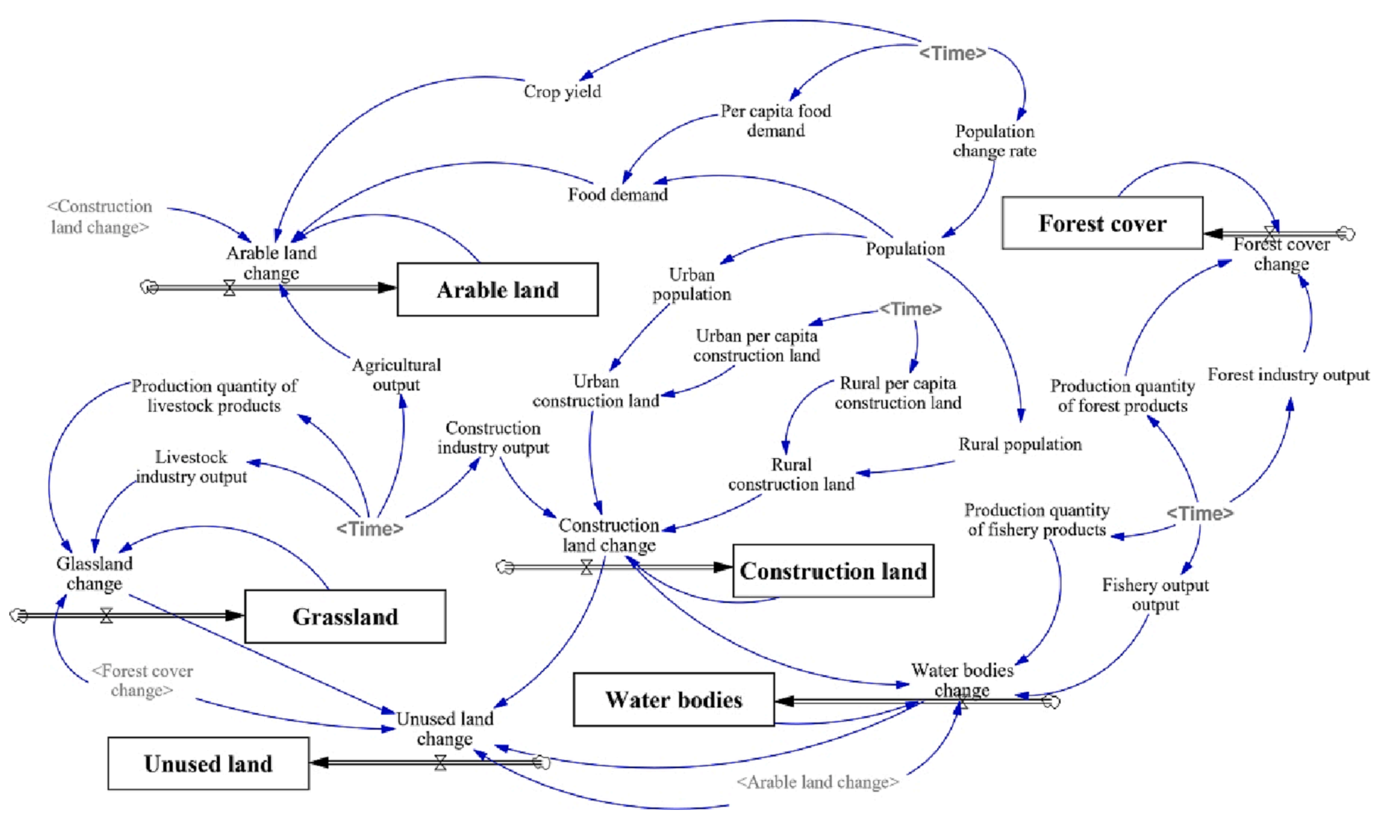

Fig. 4. SD model structure diagram.

ecological land areas of at least 5205 km^2, for ecological use; the demand for construction land decreased, and the per capita housing requirement area decreased by 8 %; protecting capital arable land; reducing the adverse impact of the disorderly extension of urban space on the ecosystem; and prohibiting development in nature reserves and national parks.

3.5. Assessment of ESV

The equivalent coefficient method was extensive applied in ESV evaluation owing to its simplicity, efficiency and applicability (Costanza et al., 1997). Xie et al. (2017) revised the equivalent coefficient of different ecosystems, its value was determined to be equal to 1/7 of the market value of the average grain output of that year. Consequently, the value coefficient of the ecosystem per unit area is obtained applying the following formulas:

$$VC = \frac{1}{7}\sum_{i=1}^{n} \frac{P_i \times Q_i}{M} \tag{1}$$

where VC is the worth of the ES equivalence factor per elemental area (CNY/ha), i refers to the kind of crop (consists of maize, wheat and rapeseed), P_i means the average market value of agricultural products (CNY/t), Q_i refers output of agricultural products per elemental area (t/ha/a), and M means overall sown acreage (ha).

$$VC_{i,j} = e_{ij} \times VC \tag{2}$$

where $e_{i,j}$ is the equivalent worth per elemental area of ES and $VC_{i,j}$ is the value coefficient of different land utilization sorts and different ES features (CNY/ha).

Various land utilization sorts, ES features and total ESVs were calculated by the following formulas:

$$ESV_i = \sum_{j=1}^{m} A_i \times VC_{i,j} \tag{3}$$

$$ESV_j = \sum_{i=1}^{n} A_i \times VC_{i,j} \tag{4}$$

$$ESV = \sum_{i=1}^{n} \left(\sum_{i=1}^{n} VC_{i,j} \right) \times A_i \tag{5}$$

where ESV_i is the ESV of land utilization form i, ESV_j is the ESV of ES j, ESV is the general ESV, and A_i is the acreage of land utilization type i.

3.6. Sensitivity index of ESV

The response of ESV to land utilization transformation was analyzed by the sensitivity indicators (SI) (Song and Deng, 2017), which can measure the impact of 1 % land utilization transformation on ESV. The larger the absolute value of SI is, the more obvious the influence of land utilization transformation on ESV is. A positive SI demonstrates that land utilization transformation improves ESV, while a negative SI suggests that land utilization transformation plays a role in reducing ESV.

$$SI = \frac{(ESV_{end} - ESV_{start})/ESV_{start} \times 100\%}{LCP} \tag{6}$$

$$LCP = \frac{\sum_{i=1}^{6} \Delta A_i}{\sum_{i=1}^{6} A_i} \times \frac{1}{T} \times 100\% \tag{7}$$

where SI is the sensitivity index (%), ESV_{start} is the total ESV of the starting year (CNY), ESV_{end} is the total ESV of the ending year (CNY), LCP refers the dynamic degree of land utilization (%), and T means the total number of years studied.

3.7. CLUE-S and CA-Markov model

CLUE-S is a predictive and visual land utilization alteration model developed by Wageningen University in the Netherlands. It iteratively achieves the spatial allocation of land application by calculating the relationship between driving forces and land types (Verburg and Overmars, 2009). The model is composed of two independent parts: non-spatial demand module and spatial allocation module. The non-spatial demand module operates independently of the model. It is necessary to employ mathematical tools such as SPSS to determine the rationality of selected land requirement, land policy and transfer restriction area (Liao et al., 2022). The spatial allocation module calculates the land utilization conversion probability in accordance with the input grid data, and allocates the land application demand in the simulated year in line with the obtained probability. The iterative process is applied to achieve the target demand of each land utilization variety. In order to execute higher simulation precision, it is necessary to enhance the conversion elasticity and transfer matrix through relevant professional knowledge, experience and multiple tests (Peng et al., 2021).

The CA-Markov model is developed on the grounds of the Markov. The Markov can only effectively simulate the quantitative relationship of land utilization variation, and has limited utility in space assignment. The state at any time node in the alteration process only relies on the results before this time point, that is, there is no aftereffect (Mokarram et al., 2021). The CA model can generate transformation rules in view of driving factors and land utilization data. The Markov model coupled with the CA model not only retains the superiority of accurate forecast of Markov model in long time series, but also integrates the benefits of CA model in simulating complex spatial and temporal alterations, and adds geospatial significance to the forecasting results of Markov model (Sun et al., 2021). The IDRISI software developed by Clark Lab is employed to generate the land utilization transfer matrix on the basis of the land application data of the two phases, and then the adaptive probability atlas is generated through the CA circular utilization driving force and land utilization information to effectively forecast the future land application variation (Zhao et al., 2019).

4. Results

4.1. Model performance evaluation

To accurately assess the precision of the MCCA model, we used the land use in 2000 as the benchmark graph and obtained the simulation results of the space pattern of land utilization in 2015 by inputting change probability, conversion rules, demand module, spatial constraints and simulation parameters of land application data in 2000–2015, as well as the driving factors such as geography, climate and socioeconomic. OA (0.9834), mcFoM (0.27) and average RE (0.574) were adopted to validate the similarity between mimetic and real land utilization configuration. Fig. 5 reveals that the real and mimetic land utilization configurations are similar in most regions, but the areas with significantly different patterns were mainly located around cities, at the boundaries of districts and counties, and along the routes of new roads. In general, the simulation results of the MCCA model are reliable and acceptable and can be employed to predict the NIS, EDS and EPS in 2030.

The SD model has been debugged and operated normally, which means that there is no logical error in the formula construction. Comparing the results of the simulated land utilization quantity in 2015 obtained by the model with the actual situation in 2015, the relative error between the simulated and actual quantity of each land utilization type is less than 1.3 %, which proves that the quantitative relationship obtained by the SD model simulation can be utilized to forecast multiple scenarios in 2030, and the model has high precision. It illustrates that SD-MCCA model can be applied for future land use scenarios prediction and ESV evaluation.

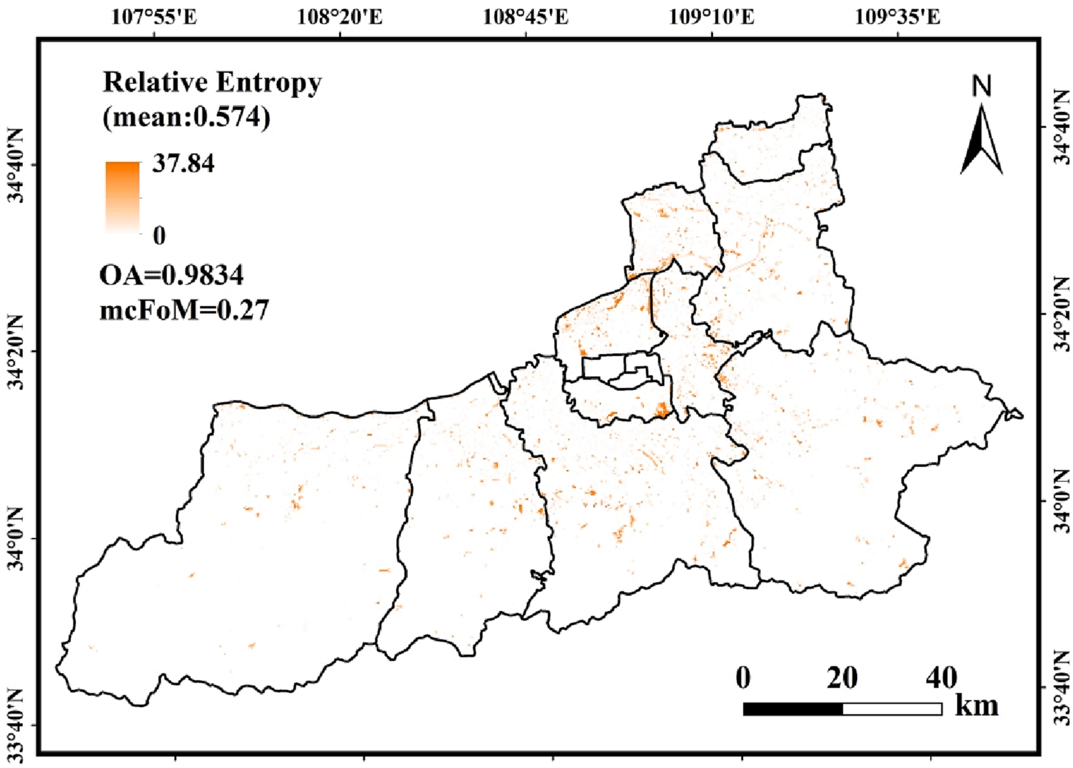

Fig. 5. Validation performance of the MCCA model.

4.2. Spatiotemporal characteristics of land utilization variations

4.2.1. Investigation of land application transformations in Xi'an during 2000–2015

Fig. 6 shows the spatial distribution of land utilization in Xi'an in 2000–2015 and reveals the evolution characteristics of various land use types with a Sankey diagram. From the perspective of spatial variation, the land use indicated significant heterogeneity in 2000 and 2015, and construction land was mainly located in the central regions, demonstrating a trend of rapid urban expansion. The arable land was mainly distributed around the built-up area, and the occupation of built-up area was the chief cause of decrease. The forest cover and meadowland areas were mainly located at south and southeast zones, and water bodies and unused land were sparsely distributed. The Sankey diagram emphasized that land utilization transformation pattern during 2000–2015 was primarily the transfer between arable land and construction land. Area of construction land converted from arable land was 438.84 km^2, accounting for 34.29 % of the area of construction land. The second reason for the decrease was the mutual transformation between arable land and grassland; the area from grassland to arable land was 60.54 km^2, accounting for 1.72 %.

4.2.2. Future scenario prediction

The land use distribution pattern under different scenarios in 2030 was predicted using the SD-MCCA model, RGB images were generated by mixing various land use structures to display more detailed simulation results (Fig. 7), and the area of various land application categories under three situations was counted (Fig. 8). The spatial pattern of land utilization in Xi'an was essentially consistent with various scenes, but there are distinctions in some parts. Compared with 2015, under the NIS, the construction land increased by 30.52 %, while the arable land, forestland and grassland exhibited a declining trend. The spatial distribution of the increase in construction land was basically in accordance with the decrease in arable land. Under the EDS, the construction land increased sharply, and the regional economy developed rapidly. The maximum growth of construction land occurs in the EDS, but the area of cropland, wood land and bare land is the lowest in the three future prediction scenarios. On the premise of ensuring sufficient arable land to guarantee food production, arable land, grassland and unused land were reduced by 14.91 %, 2.36 % and 9.28 %, respectively. Under the EPS, the acreage of built-up area was the slowest, increased by 357.36 km^2, but the area of forest cover reached a maximum of 3072.91 km^2 among the three scenarios. The area of arable land was less than that in the NIS but higher than that in the EDS, indicating that the implementation of the ecological protection policy has restrained urban sprawl and strengthened protection of arable land.

4.3. Changes in ESV from 2000 to 2030

4.3.1. Temporal estimation in ESV

From 2000 to 2030, the ESV in Xi'an demonstrated a tendency of first rising, then falling and finally growing again, with an overall increasing trend (Table 1 and Table 2). The highest ESV under the EPS was largely due to the protection and restoration of ecological land and the restriction of disorderly urban sprawl, while the lowest ESV under the EDS was mainly driven by the acceleration of industrialization and urbanization and the continuous expansion of the scale of construction land. From 2000 to 2015, the total ESV increased, with a gain of 1.32×10^6 CNY, and further increased by 3.29×10^6 CNY and 62.72×10^6 CNY in NIS and EPS during 2015–2030; however, the general ESV for EDS decreased sharply, reduced by 321.85×10^6 CNY, indicating that urban expansion has a serious negative influence on ESV. Forest cover, grassland and water bodies had the highest contributions of 88.84 % – 91.42 % to the ESV, while the proportion of unused land was the lowest. The ESV of arable land and grassland revealed decreasing trends in 2000–2015, while the ESV of forest cover, water bodies and unused land displayed increasing trends to varying degrees. The ESV of arable land and grassland continued to decrease from 2015 to 2030; nevertheless, water bodies exhibited an overall growth trend, but forest cover and unused land demonstrated significant differences under different

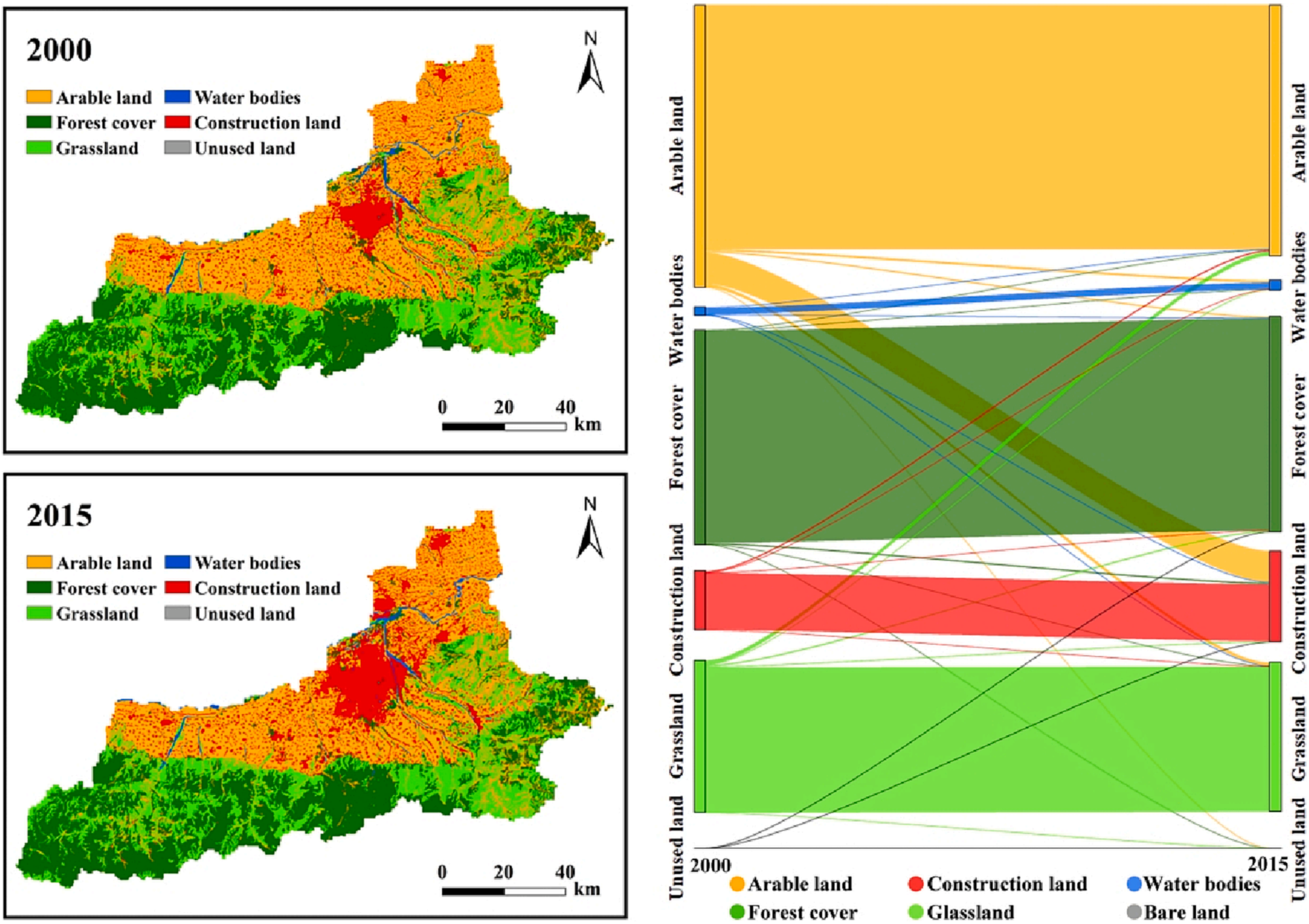

Fig. 6. Space distribution of land utilization and Sankey diagram during 2000–2015.

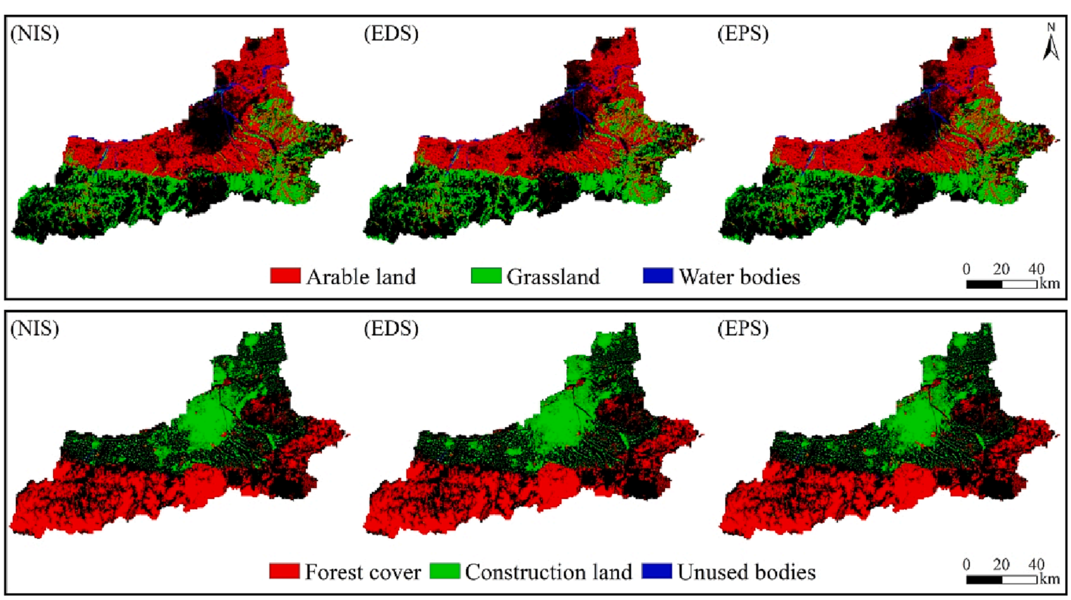

Fig. 7. Mixed distribution of land utilization structures under different scenarios in 2030 in view of RGB images.

scenarios. The ESV of forest cover increased in NIS and EPS, whereas decreased in EDS (-51.77$\times$10^6 CNY). The ESV of unused land under EDS and EPS decreased, while the ESV under NIS increased.

The proportion of ESV provided by different ecosystem services from 2000 to 2030 is shown in Fig. 9. Generally, there was little change in the proportions of ESV of each function, which demonstrated that the

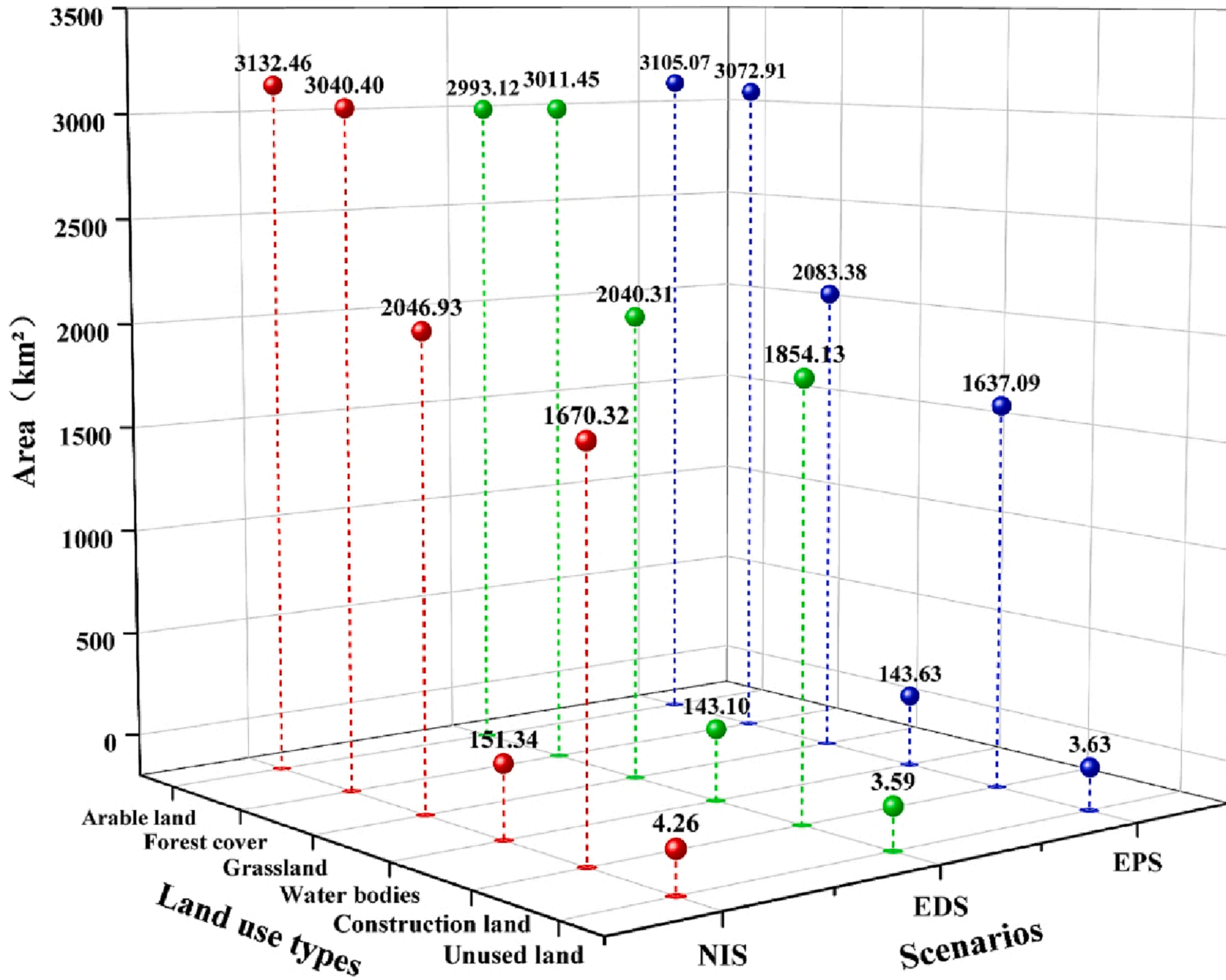

Fig. 8. Acreage of different land utilization forms under various scenarios in 2030.

Table 1
ESV and proportion of various land use during 2000–2030 (uint:10^6 CNY).

Year	Scenario	Factor	Arable land	Forest cover	Grassland	Water bodies	Unused land	Total
2000		ESV	2182.29	9588.65	5839.87	1943.26	0.29	19554.36
		Percentage	11.16 %	49.04 %	29.86 %	9.94 %	0.00 %	100.00 %
2015		ESV	1939.07	9638.81	5715.23	2262.22	0.35	19555.68
		Percentage	9.92 %	49.29 %	29.23 %	11.57 %	0.00 %	100.00 %
2030	NIS	ESV	1726.84	9705.71	5598.31	2527.73	0.38	19558.97
		Percentage	8.83 %	49.62 %	28.62 %	12.92 %	0.00 %	100.00 %
	EDS	ESV	1650.02	9613.30	5580.22	2389.97	0.32	19233.83
		Percentage	8.58 %	49.98 %	29.01 %	12.43 %	0.00 %	100.00 %
	EPS	ESV	1711.74	9809.48	5698.02	2398.84	0.32	19618.39
		Percentage	8.73 %	50.00 %	29.04 %	12.23 %	0.00 %	100.00 %

Table 2
ESV change rate by different land use from 2000 to 2030.

Year	Scenario	Factor	Arable land	Forest cover	Grassland	Water bodies	Unused land
2000–2015		Change rate	−11.15 %	0.52 %	−2.13 %	16.41 %	22.15 %
2015–2030	NIS		−10.95 %	0.69 %	−2.05 %	11.74 %	7.57 %
2015–2030	EDS		−14.91 %	−0.26 %	−2.36 %	5.65 %	−9.28 %
2015–2030	EPS		−11.72 %	1.77 %	−0.30 %	6.04 %	−8.46 %

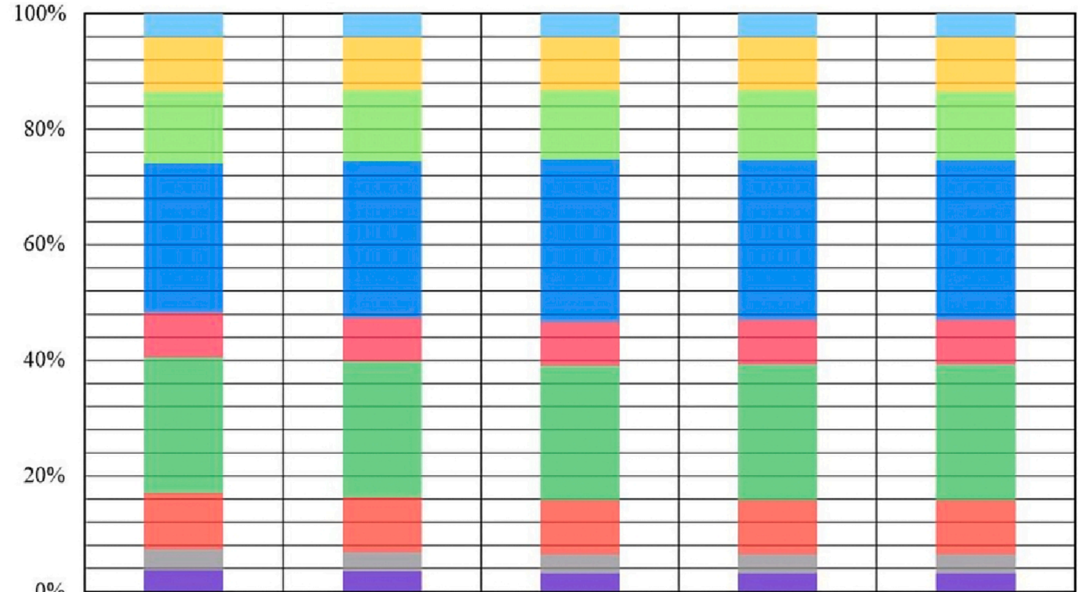

	2000	2015	2030（NIS）	2030（EDS）	2030（EPS）
Landscape aesthetics	810.711	808.225	806.535	797.844	814.114
Biodiversity protection	1809.846	1799.862	1792.430	1774.855	1811.594
Soil conservation	2460.117	2388.273	2327.193	2292.460	2346.879
Hydrological regulation	5036.811	5283.793	5491.404	5342.757	5419.730
Waste treatment	1497.422	1499.411	1501.791	1483.686	1513.150
Climate regulation	4606.812	4571.146	4544.268	4502.717	4597.499
Gas regulation	1918.289	1870.352	1829.837	1804.822	1846.649
Raw material production	682.106	655.436	632.582	621.121	636.731
Food production	732.242	679.181	632.930	613.564	632.050

Fig. 9. Proportion of ESV with different ecosystem services from 2000 to 2030.

structures of ecosystem service functions were relatively stable in different periods. Hydrological and climate regulation were the dominant functions, contributing 49.31 %-51.31 % of general ESV. By comparison, primary material and grain yields were the lowest contributors, accounting for 6.42 % – 7.23 % and having little influence on ESV. The ESV of hydrologic regulation and waste treatment increased from 2000 to 2015, while the remaining ecosystem services indicated a decreasing trend. The ESVs of various functions under the NIS and EPS were higher than those under the EDS. In addition, the ESV of hydrologic regulation and food production under the NIS was larger than that under the EPS, but the ESVs of other functions were lower than those under the EPS. Compared with 2015, the ESV and growth rate of hydrological regulation reached the maximum under the NIS, which were 5491.40×10^6 CNY and 3.93 %, respectively. The ESV of landscape aesthetics was the

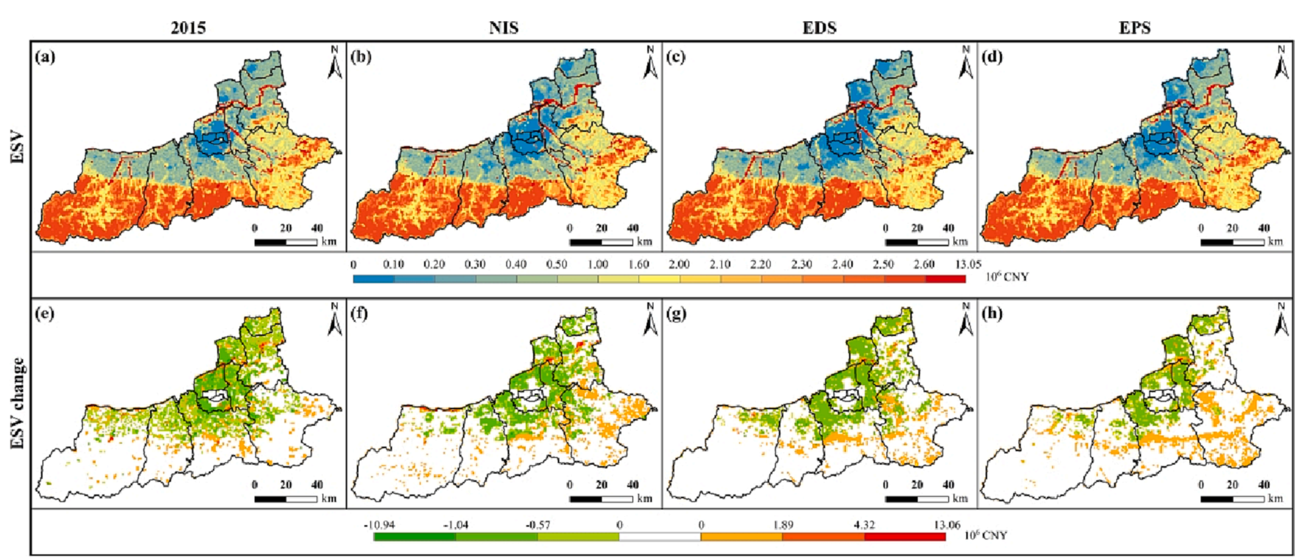

Fig. 10. Spatial distribution and changes in ESV. (a-d refers to the spatial distribution of ESV in 2015, NIS, EDS and EPS, respectively, and e-h is the changes during 2000–2015, 2015-NIS, 2015-EDS and 2015-EPS, respectively.).

highest and presented an increasing trend under the EPS, while it decreased under the other scenarios. The ESV of food production decreased most significantly under the EDS (-65.62×10^{6} CNY) and the maximum variation range (-9.66 %).

4.3.2. Spatial characteristics of ESV

The spatial distribution and change details of ESV under the three scenarios in Xi'an during 2015–2030 are shown in Fig. 10. The distribution pattern of ESV was basically stable in different periods, but there were differences between regions. Spatial pattern of ESV was highly consistent with land utilization forms. Medium-high ESVs were mostly located in woodland and meadowland with good natural conditions, although low-value areas were chiefly located in northern Zhouzhi, Huyi and Changan, as well as in most areas of Gaoling, Lintong and Yanliang, which was consistent with the distribution of arable land. The ESVs in the urban center and surrounding areas were the lowest. Compared with the ESV in 2000–2015, the losses of ESV under EDS were the largest, indicating characteristic decreases in high value areas and increases in low value areas, mainly owing to the pursuit of economic benefits and urban development. ESV gains were enhanced and losses were reduced under NIS; nevertheless, the ESV benefits were the highest and the losses were the lowest under the EPS, which was mainly due to the strict ecological protection policies in that scenario. The results were essentially in accordance with those of Wuhan (Wang et al., 2018a).

4.4. Zoning statistics of ESV in Xi'an

The radar map in Fig. 11 displays the proportion of ESV in all the

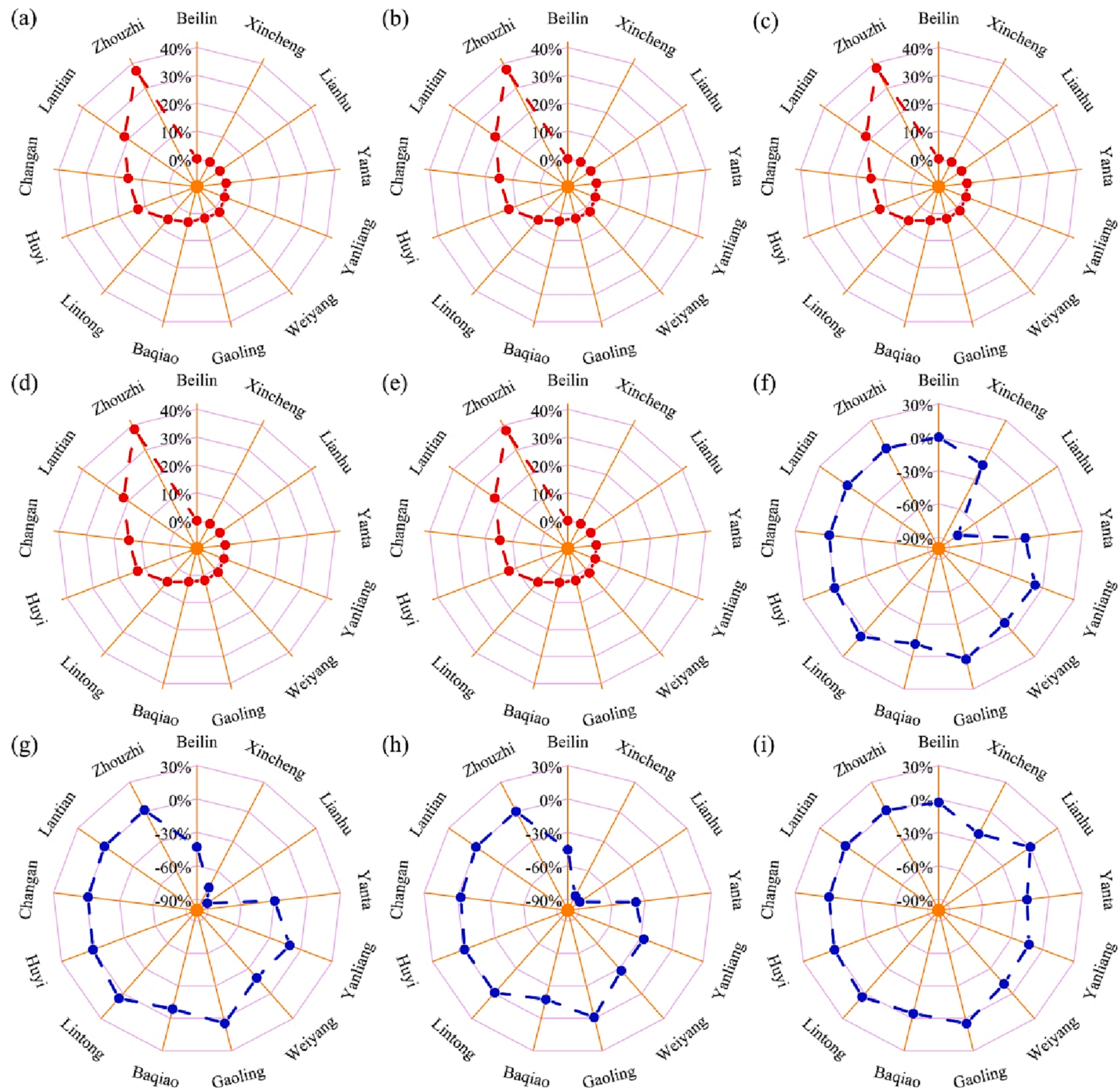

Fig. 11. Radar map of ESV changes in districts and counties in Xi'an from 2000 to 2030. (a-e refer to the results in 2000, 2015, and the NIS, EDS and EPS, respectively, and f-j is divided into changes in different periods).

districts and counties of Xi'an. On the whole, the ESV was similar in different periods, but there were great differences in the same period (Fig. 11). Zhouzhi, Lantian and Changan provided the highest proportion of ESV, which was more than 14.52 %, while the lowest proportion was found in Lianhu, Xincheng and Beilin, which was less than 0.02 %. The closer to the downtown area, the lower the ESV of the districts and counties with higher urbanization levels, and vice versa. From 2000 to 2015, Lintong saw the largest increase in ESV of 5.71 %, while Lianhu saw the most significant decrease of 79.24 %. From 2015 to 2030, the ESV of Beilin and Xincheng diminished significantly under the NIS, mainly due to the lower ESV and the larger variation caused by smaller numerical changes. In comparison, the reduction in the EDS was more obvious, mainly because of rapid economic development and intensified human activities. Nonetheless, in the EPS, the ESV of all districts and counties tended to be stable and exhibited an overall upward trend, mainly as a result of the contribution of strict ecological restoration and protection policies.

4.5. SI of ESV to land utilization variations

To further reveal the influence of land application dynamics on ESV in different periods of Xi'an, we calculated and plotted the spatiotemporal distribution of SI (Fig. 12). The SI of Xi'an in 2000–2015 was 0.007, implying that the land utilization evolution had an active role in ESV during this period. In 2015–2030, SI varied greatly under different scenarios. SI increased slightly under NIS (0.024) but increased significantly under EPS (0.508), while it declined significantly under EDS (-1.744). This suggested that land application transformation had an active role in ESV under NIS and EPS, while under EDS, ESV had a negative response to land use spatial differentiation, which was consistent with the findings of Peng et al. (2021). The physical significance of SI revealed that a 1 % change in land use structure in the historical period and NIS would result in approximately 0.007 % and 0.024 % changes in ESV, respectively. However, under EPS, a 1 % increase in forest cover would give rise to a 2.718 % increase in ESV, while under EDS, a 1 % decrease in arable land would cause a 1.656 % decrease in ESV. This result suggested that ESV was sensitive to land use transition. The spatial distribution of low SI regions in 2000–2015 was similar to that in the three predicted scenarios, which was predominantly concentrated in the central and surrounding areas, chiefly owing to rapid urbanization, demonstrating that ESV in these regions had a negative response to land use change. In contrast, the high SI areas were different and revealed a scattered distribution, but the SI under NIS and EPS was relatively high, primarily since the transformation of land use types with a low value coefficient to ecological land with a high value coefficient and the land use evolution in these zones had a beneficial impact on ESV.

4.6. Comparison with simulation results of existing models

MCCA model can effectively forecast future land utilization variation and has remarkable superiority in land application prediction. In order to confirm the simulation performance of MCCA model, two land use prediction models CA-Markov and CLUE-S with widely demonstrated accuracy were selected. According to the same land utilization data of Xi'an in 2000 and the driving forces such as geography, climate and social economy required by MCCA, the results of urban expansion and alteration in Xi'an in 2015 were simulated. While comparing the overall simulation results of MCCA, CLUE-S and CA-Markov models, it is necessary to investigate the details of changes in specific locations. Fig. 13 exhibits the actual spatial pattern of land use in Xi'an in 2015 and the distribution condition of land utilization in 2015 simulated by MCCA, CA-Markov and CLUE-S respectively, and selects three characteristic regions for analysis to comprehensively show the differences of the models. The results show that the precision of MCCA model is still significantly higher than that of CA-Markov model and CLUE-S model, although the space distribution of the actual observation results is similar to that of the three models. The Kappa index of the MCCA was 0.969, which was better than 0.926 and 0.854 of the CA-Markov and the CLUE-S. From a macro perspective, the MCCA model has superior simulation accuracy and has the ability to accurately simulate future land use spatial pattern variations.

Through the detailed comparison map, it can be found that there are regional differences in the prediction results of the three models, and the differences are more obvious for specific land utilization types. The detail figure c1 indicates that the simulation results of CA-Markov model show the aggregation characteristics. The prediction of construction land expansion is relatively conservative, and the simulation of land use

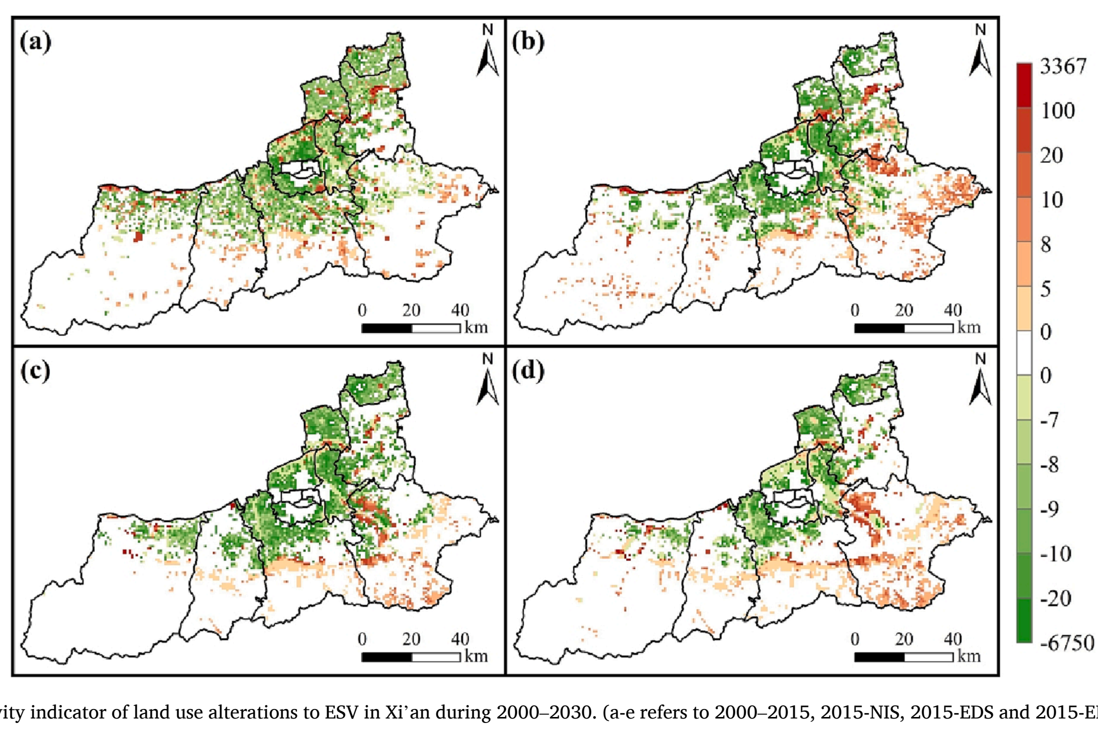

Fig. 12. Sensitivity indicator of land use alterations to ESV in Xi'an during 2000–2030. (a-e refers to 2000–2015, 2015-NIS, 2015-EDS and 2015-EPS, respectively.).

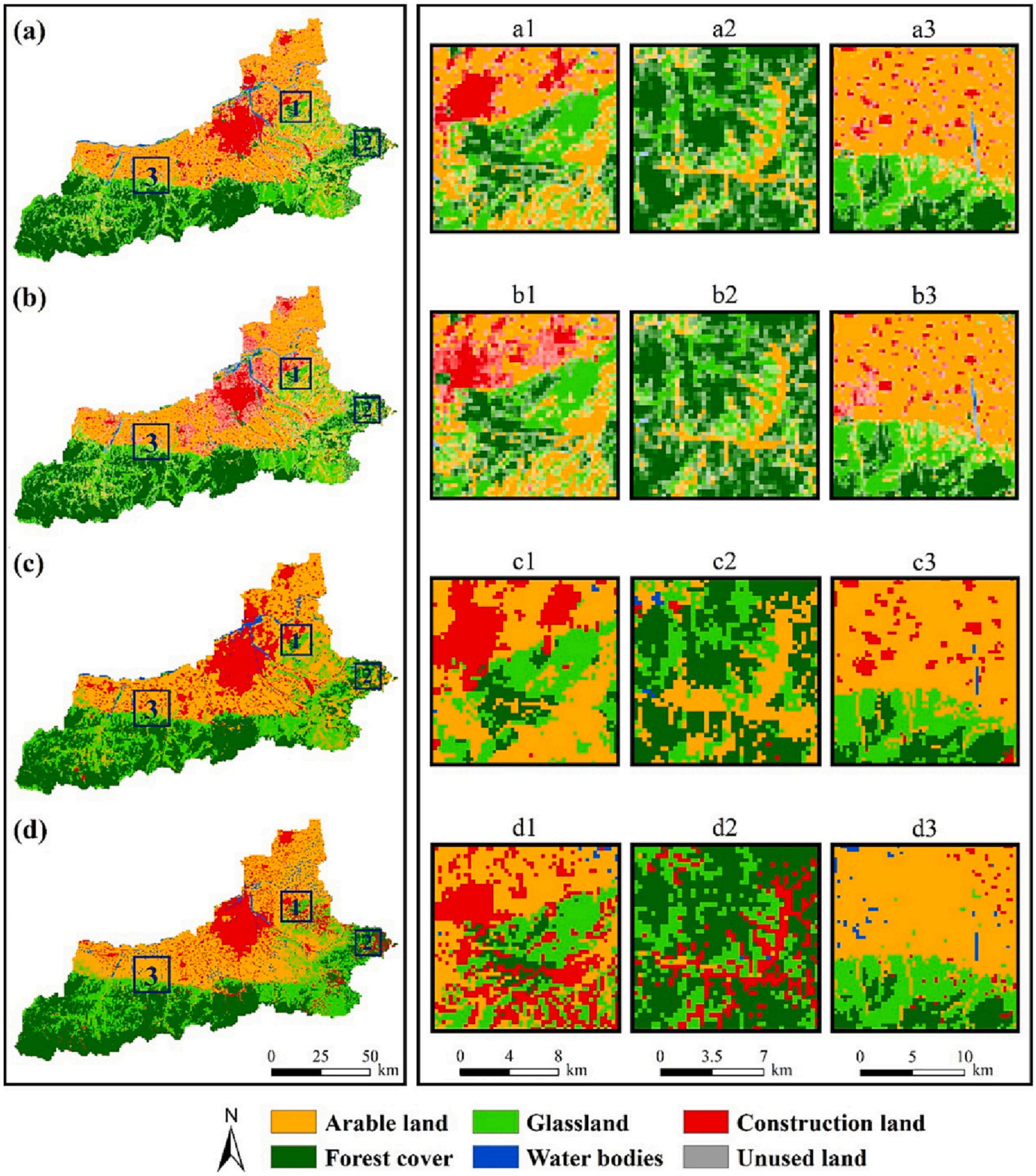

Fig. 13. Comparison between the predicted results of the spatial distribution of land use of the three models and the actual situation in 2015. (a refers to actual land utilization, b, c and d are MCCA, CA-Markov and CLUE-S models, respectively, 1–3 are three selected areas.).

distribution exhibits a relatively centralized trend. Although the overall space distribution trend can be kept similar to the actual observation results, it is difficult to obtain that a large area of land utilization type contains other independent types, which can be further confirmed in the c3 diagram. D1, d2 and d3 can clearly display that the CLUE-S model is more difficult to constrain the disorderly expansion of land utilization types, and there is a phenomenon that the predicted alterations are not consistent with the actual situation in some parts, especially the outcomes presented by d1 and d2. The construction land encroaches on the cultivated land excessively, resulting in a significant difference between the simulation outcomes and the actual situation. Compared with CA-Markov and CLUE-S, MCCA shows stable and superior performance in both spatial simulation and overall accuracy, and the simulation results have the smallest deviation from the actual. MCCA performs more detailed and accurate in the simulation of small patches, and is more in line with the actual land utilization situation. These characteristics not only simulate the law of urban development, but also reveal the spatial heterogeneity that the other two models cannot fully reflect. Therefore, it can be concluded that contrasted to CA-Markov and CLUE-S, MCCA can more precisely and carefully reflect the urban variation process of Xi'an and reveal its internal mechanism.

5. Discussion

5.1. A new approach for predicting future ESV

In this research, the novel mixed-cell MCCA model and system dynamics SD model were established that considered the actual land utilization and drivers. Equivalent coefficient method was adopted, then three future land use scenarios were introduced to predict the spatial-temporal heterogeneity response of ESV, to investigate the impact of land application dynamic transformation on ESV, and provide a new method for future land utilization simulation and ESV prediction. Compared with the traditional pure-cell CA model, the land use competition and transformation rules of the MCCA model were founded on the mixed information contained in the pixels, which can describe the dynamic evolution of land use at the subpixel level and help researchers fully investigate the interaction between multiple driving forces (Liang et al., 2021). The prediction results were converted from pure and one-dimensional to mixed and multidimensional, making the results more rational. In terms of simulation accuracy, MCCA has a high reliability and strong robustness. Since the transformation rules of MCCA emphasize more competition and conversion on the subpixel scale than conventional models, it can still simulate subtle variations for land use types with small demand alterations (Zhou and Peng, 2022). The MCCA has achieved quantitative and continuous simulation of changes in various land use components in pixels, solved the long-standing difficulties of the pure-cell model, and obtained more accurate and detailed prediction results of land use space distribution, realizing the leap from qualitative to quantitative forecasting. In summary, MCCA can predict the future pattern of land utilization more realistic. In addition, it also has all the functions of the pure-cell model because it can alter the mixed structure into the traditional discrete model (Liang et al., 2021). The combination of SD model and MCCA model can give full play to the advantages of quantitative structure optimization and spatial dynamic simulation, and can deeply reveal the spatiotemporal characteristics of land use change and the ESV response mechanism.

5.2. Comparison results with previous studies

This study employs SD-MCCA model to forecast the alteration of ESV in the future under multiple scenarios in Xi'an, which plays a very significant role in the formulation of sustainable development policies and the exploration of innovative methods of land utilization simulation. Shao et al. (2020) and Li et al. (2020) explored the dynamic changes of ESV in Xi'an, the spatial pattern of ESV was basically consistent with this research, the low ESV regions were mainly concentrated in the urban center and surrounding zones. In addition, the influence mechanism of land application scenarios in different areas on ESV was also essentially similar to that of this study (Kulsoontornrat and Ongsomwang, 2021).

The land utilization prediction model directly determines the precision of urban spatial layout simulation, and ultimately affects the response of ESV. Gashaw et al. (2018) applied the CA-Markov model to forecast land utilization variation and assess the response of ESV in the Upper Blue Nile basin of Ethiopia (Kappa = 0.83). The researchers used the CA model optimized by random forest to evaluate the ESV of Qingdao metropolitan zone (Qin and Fu, 2020) (Kappa = 0.86). The CLUE-S model has been employed by some scholars to investigate the spatiotemporal transformations of ESV in Jiangsu Province (Wu et al., 2020) (Kappa = 0.95). Li et al. (2021) utilized the PLUS model to reveal the variation mechanism of ESV in the Sichuan-Yunnan ecological barrier (Kappa = 0.87). Ma and Wang (2022) exploited the Markov-FLUS model to examine the alterations of ESV under the multiple scenarios of Wuhan Metropolitan Area (Kappa = 0.952). Contrasted with previous researches, this study adopted the SD-MCCA model to forecast the response of ESV to land utilization variation (Kappa = 0.969), and the accuracy was significantly enhanced compared with the traditional model, and the simulation results were more in line with actual changes.

The SD-MCCA model takes into account the control of land utilization quantity and the optimization of spatial distribution, which is a novel way to probe the dynamic changes of urban development pattern and ESV. Wang et al. (2022b) and Zhao et al. (2022) optimized land use simulation according to SD model, and both Kappa reached 0.93, implying that it is feasible for SD model to improve land application simulation model. However, most studies are limited to land use prediction, and few are further used for ESV exploration. The coupled SD-MCCA model can not only ensure the reasonable quantitative relationship between land utilization types, but also realize the optimization of spatial distribution. The combined model has stronger performance and robustness.

5.3. Suggestions for policy-making

Evaluating the dynamics of ESV under various scenarios in the future can quantify the variations in economic value corresponding to land use change and provide references for government decision makers to coordinate ecological construction and economic growth and achieve sustainable development (Hou et al., 2020). First, determining the optimal land application configuration is the key to improve ecological benefits and achieve the goal of maximizing ESV, and urbanization is the crucial factor affecting ESV changes (Jiang et al., 2020). In the future, land use management should achieve both economic and environmental benefits. Rational planning of land utilization allocation by clarifying the ecological and arable land red lines and urban growth boundary, to prevent excessive encroachment on ecological land in the development process (Chen et al., 2021b). Second, the government should promptly monitor the land use dynamics in areas with significant ESV alterations. For instance, in the hot spot region of ESV conversions in Zhouzhi, more ecological land should be developed to strengthen social and economic benefits, while Beilin, a cold spot zone, should consider slowing the development trend. Third, the government needs to emphasize planning, adhere to ecological protection, green and low-carbon principles, and transform traditional development with its low output, heavy pollution and recycling difficulties into a green development system with high efficiency, low emissions and resource regeneration. Furthermore, due to the significant spatial spillover effect between urban districts and counties (Bai et al., 2018), regional environmental protection cooperation needs to be further improved. Additionally, government decision makers should focus on solving the problems caused by the degradation of ecosystem service functions, follow the rules of natural and economic development, convey the concept of resource conservation and the recycling economy to the public, and promote public participation in social governance.

5.4. Limitations and future research

The MCCA model was successfully adopted to predict the changes and heterogeneity of ESV under three future scenarios in Xi'an, but it still had some limitations. Scenario prediction applies a land use transfer matrix and government planning policies and does not fully consider the impact of climate change, social and economic indicators and other factors (Long et al., 2022). In the future, the MCCA method can be combined with gray model (Wang et al., 2022b) and integrated with representative concentration pathways (RCPs), Sustainable Development Goals (SDGs), and shared socioeconomic pathways (SSPs) and to quantitatively obtain land application request and model the land utilization pattern in multiple scenarios (Zhang et al., 2022), improve the simulation accuracy and further explore the response mechanism of ESV. The value coefficient approach ignores the difference in crop prices in different periods, which leads to a static estimation of ESV. It also does not fully consider the complexity of ecosystem types and people's incomes and consumption levels. The accuracy of ESV assessment can be improved through crop price prediction, value coefficient correction and ESV spatial optimization (Hu et al., 2019; Ling et al., 2019). The spatial distribution and variation in ESV are explored by combining the new MCCA model with the SD model, and the uncertainty generated by different driving force input data and various urban expansion models has not been compared, which will be an important research direction for ESV in the future.

6. Conclusion

We developed an innovative MCCA model and coupled it with the system dynamics SD model, combined with the equivalent coefficient method to forecast the future land utilization spatial pattern, and investigated variations and sensitivity of ESV under different scenarios from 2000 to 2030. OA (0.9834), mcFoM (0.27) and average RE (0.574) indicated that the MCCA model had high simulation accuracy and stable performance. Land application transformation revealed rules of construction land expansion, a slight increase in woodland and cropland degradation in 2000–2015. The variation trend under the NIS was consistent with the historical trends, while the acreage of built-up area was the largest under EDS, whereas increase in forest cover was the most obvious under the EPS. ESV generally exhibited an increasing trend. ESV in NIS and EPS enhanced by 3.29×10^{6} CNY and 62.72×10^{6} CNY during 2015–2030, respectively, but decreased by 321.85×10^{6} CNY under EDS. The benefits of ESV were primarily because of protection and restoration of ecological land, and decreases were largely result of the acceleration of urbanization and industrialization. Hydrological and climate regulation accounted for the largest proportion of ESV. The SI under the NIS and EPS were 0.024 and 0.508, respectively, demonstrating land utilization variation had an active impact on ESV, although SI in EDS was -1.744, implying that ESV had a negative response to land use transformation and that ESV was more sensitive to forest cover and arable land variety. This study employed a novel method SD-MCCA for land use variations and ESV prediction, which has important theoretical and practical significance for urban sustainable planning, as well as ecological compensation policies. In future studies, combination of MCCA with InVEST and other ecological models will contribute to the accurate assessment and spatial optimization of ecosystem services.

CRediT authorship contribution statement

Ping Zhang: Conceptualization, Methodology, Writing – original draft, Writing – review & editing, Funding acquisition. **Lei Liu:** Conceptualization, Methodology, Software, Validation, Writing – original draft, Writing – review & editing. **Lianwei Yang:** Methodology, Software, Data curation. **Juan Zhao:** Methodology, Data curation. **Yangyang Li:** Data curation, Validation. **Yuting Qi:** Methodology, Data curation. **Xuenan Ma:** Data curation, Visualization. **Lei Cao:** Software, Validation.

Declaration of Competing Interest

The authors declare that they have no known competing financial interests or personal relationships that could have appeared to influence the work reported in this paper.

Data availability

Data will be made available on request.

Acknowledgments

This research was supported by the Natural Science Basic Research Program of Shaanxi (Program No. 2021JM-447), the Opening Fund of State Key Laboratory of Green Building in Western China (LSKF202309), the Project funded by China Postdoctoral Science Foundation (2017M610119), the Fund Project of Shaanxi Key Laboratory of Land Consolidation (2018-JC12), and the Fund Project of Xi'an Key Laboratory of Territorial Spatial Information (2023).

References

Akhtar, M., Zhao, Y.Y., Gao, G.L., Gulzar, Q., Hussain, A., 2022. Assessment of spatiotemporal variations of ecosystem service values and hotspots in a dryland: A case-study in Pakistan. LDD 33, 1383–1397.
Arowolo, A.O., Deng, X., Olatunji, O.A., Obayelu, A.E., 2018. Assessing changes in the value of ecosystem services in response to land-use/land-cover dynamics in Nigeria. Sci. Total Environ. 636, 597–609.
Aziz, T., 2021. Changes in land use and ecosystem services values in Pakistan, 1950–2050. Environmental Development 37, 100576.
Bai, Y.P., Deng, X.Z., Jiang, S.J., Zhang, Q., Wang, Z., 2018. Exploring the relationship between urbanization and urban eco-efficiency: Evidence from prefecture-level cities in China. Journal of Cleaner Production 195, 1487–1496.
Bateman, I.J., Harwood, A.R., Mace, G.M., Watson, R.T., Abson, D.J., Andrews, B., Binner, A., Crowe, A., Day, B.H., Dugdale, S., Fezzi, C., Foden, J., Hadley, D., Haines-Young, R., Hulme, M., Kontoleon, A., Lovett, A.A., Munday, P., Pascual, U., Paterson, J., Perino, G., Sen, A., Siriwardena, G., van Soest, D., Termansen, M., 2013. Bringing ecosystem services into economic decision-making: land use in the United Kingdom. Sci 341, 45–50.
Camacho-Valdez, V., Ruiz-Luna, A., Ghermandi, A., Berlanga-Robles, C.A., Nunes, P., 2014. Effects of land use changes on the ecosystem service values of coastal wetlands. Environ. Manage. 54, 852–864.
Chen, W., Zeng, J., Zhong, M., Pan, S., 2021a. Coupling analysis of ecosystem services value and economic development in the Yangtze River economic belt: a case study in Hunan Province. China. Remote Sensing 13, 1552.
Chen, W.X., Zeng, J., Chu, Y.M., Liang, J.L., 2021b. Impacts of landscape patterns on ecosystem services value: a multiscale buffer gradient analysis approach. Remote Sensing 13, 2551.
Collin, M.L., Melloul, A.J., 2001. Combined land-use and environmental factors for sustainable groundwater management. Urban Water 3, 229–237.
Costanza, R., dArge, R., deGroot, R., Farber, S., Grasso, M., Hannon, B., Limburg, K., Naeem, S., Oneill, R.V., Paruelo, J., Raskin, R.G., Sutton, P., vandenBelt, M., 1997. The value of the world's ecosystem services and natural capital. Nature. 387. 253-260.
Dai, X.A., Johnson, B.A., Luo, P.L., Yang, K., Dong, L.X., Wang, Q., Liu, C., Li, N.W., Lu, H., Ma, L., Yang, Z.L., Yao, Y.Z., 2021. Estimation of urban ecosystem services value: a case study of Chengdu. Southwestern China. Remote Sensing 13, 207.
Das, S., Shit, P.K., Patel, P.P., 2021. Ecosystem services value assessment and forecasting using integrated machine learning algorithm and CA-Markov model: an empirical investigation of an Asian megacity. GeoIn 49, 2002424.
de Groot, R.S., Alkemade, R., Braat, L., Hein, L., Willemen, L., 2010. Challenges in integrating the concept of ecosystem services and values in landscape planning, management and decision making. Ecol. Complex. 7, 260–272.
Elmqvist, T., Setala, H., Handel, S.N., van der Ploeg, S., Aronson, J., Blignaut, J.N., Gomez-Baggethun, E., Nowak, D.J., Kronenberg, J., de Groot, R., 2015. Benefits of restoring ecosystem services in urban areas. Current Opinion in Environmental Sustainability 14, 101–108.
Fisher, B., Turner, R.K., Morling, P., 2009. Defining and classifying ecosystem services for decision making. Ecol. Econ. 68, 643–653.
Fu, J., Zhang, Q., Wang, P., Zhang, L., Tian, Y.Q., Li, X.R., 2022. Spatio-temporal changes in ecosystem service value and its coordinated development with economy: a case study in Hainan Province. China. Remote Sensing 14, 970.
Gashaw, T., Tulu, T., Argaw, M., Worqlul, A.W., Tolessa, T., Kindu, M., 2018. Estimating the impacts of land use/land cover changes on Ecosystem Service Values: The case of the Andassa watershed in the Upper Blue Nile basin of Ethiopia. Ecosystem Services 31, 219–228.
Hou, L., Wu, F.Q., Xie, X.L., 2020. The spatial characteristics and relationships between landscape pattern and ecosystem service value along an urban-rural gradient in Xi'an city. China. Ecol. Indicators 108, 105720.
Hu, M., Li, Z., Wang, Y., Jiao, M., Li, M., Xia, B., 2019. Spatio-temporal changes in ecosystem service value in response to land-use/cover changes in the Pearl River Delta. Resources Conservation and Recycling 149, 106–114.
Huang, Z.H., Li, X.J., Du, H.Q., Mao, F.J., Han, N., Fan, W.L., Xu, Y.X., Luo, X., 2022. Simulating Future LUCC by Coupling Climate Change and Human Effects Based on Multi-Phase Remote Sensing Data. Remote Sensing 14, 1698.
Jiang, W., Fu, B.J., Lu, Y.H., 2020. Assessing impacts of land use/land cover vonversion on changes in ecosystem services value on the Loess Plateau. China. Sustainability 12, 7128.
Keller, M., Jacob, D.J., Wofsy, S.C., Harriss, R.C., 1991. Effects of tropical deforestation on global and regional atmospheric chemistry. Clim. Change 19, 139–158.
Kindu, M., Schneider, T., Teketay, D., Knoke, T., 2016. Changes of ecosystem service values in response to land use/land cover dynamics in Munessa-Shashemene landscape of the Ethiopian highlands. Sci. Total Environ. 547, 137–147.
Kulsoontornrat, J., Ongsomwang, S., 2021. Suitable Land-Use and Land-Cover Allocation Scenarios to Minimize Sediment and Nutrient Loads into Kwan Phayao, Upper Ing Watershed. Thailand. Applied Sciences-Basel 11, 10430.
Letourneau, A., Verburg, P.H., Stehfest, E., 2012. A land-use systems approach to represent land-use dynamics at continental and global scales. Environ. Model. Software 33, 61–79.
Li, J.Y., Chen, H.X., Zhang, C., Pan, T., 2019. Variations in ecosystem service value in response to land use/land cover changes in Central Asia from 1995–2035. PeerJ 7, e7665.
Li, C., Wu, Y.M., Gao, B.P., Zheng, K.J., Wu, Y., Li, C., 2021. Multi-scenario simulation of ecosystem service value for optimization of land use in the Sichuan-Yunnan ecological barrier. China. Ecol. Indicators 132, 108328.
Li, X.X., Zhang, H.J., Zhang, Z.C., Feng, J., Liu, K., Hua, Y.W., Pang, Q., 2020. Spatiotemporal Changes in Ecosystem Services along a Urban-Rural-Natural Gradient: A Case Study of Xi'an. China. Sustainability 12, 1133.
Liang, X., Guan, Q., Clarke, K.C., Chen, G., Guo, S., Yao, Y., 2021. Mixed-cell cellular automata: A new approach for simulating the spatio-temporal dynamics of mixed land use structures. Landscape Urban Plann. 205, 103960.
Liao, G.T., He, P., Gao, X.S., Lin, Z.Y., Huang, C.Y., Zhou, W., Deng, O.P., Xu, C.H., Deng, L.J., 2022. Land use optimization of rural production-living-ecological space at different scales based on the BP-ANN and CLUE-S models. Ecol. Indicators 137, 108710.
Ling, H., Yan, J., Xu, H., Guo, B., Zhang, Q., 2019. Estimates of shifts in ecosystem service values due to changes in key factors in the Manas River basin, northwest China. Sci. Total Environ. 659, 177–187.
Liu, Y.B., Hou, X.Y., Li, X.W., Song, B.Y., Wang, C., 2020. Assessing and predicting changes in ecosystem service values based on land use/cover change in the Bohai Rim coastal zone. Ecol. Indicators 111, 106004.

Liu, M., Jia, Y., Zhao, J., Shen, Y., Pei, H., Zhang, H., Li, Y., 2021b. Revegetation projects significantly improved ecosystem service values in the agro-pastoral ecotone of northern China in recent 20 years. Sci. Total Environ. 788, 147756.

Liu, J.M., Xiao, B., Jiao, J.Z., Li, Y.S., Wang, X.Y., 2021a. Modeling the response of ecological service value to land use change through deep learning simulation in Lanzhou. China. Sci. Total Environ. 796, 148981.

Long, X., Lin, H., An, X., Chen, S., Qi, S., Zhang, M., 2022. Evaluation and analysis of ecosystem service value based on land use/cover change in Dongting Lake wetland. Ecol. Indicators 136, 108619.

Ma, B.W., Wang, X., 2022. What is the future of ecological space in Wuhan Metropolitan Area? A multi-scenario simulation based on Markov-FLUS. Ecol. Indicators 141, 109124.

Mendoza-Gonzalez, G., Martinez, M.L., Lithgow, D., Perez-Maqueo, O., Simonin, P., 2012. Land use change and its effects on the value of ecosystem services along the coast of the Gulf of Mexico. Ecol. Econ. 82, 23–32.

Mokarram, M., Pourghasemi, H.R., Hu, M., Zhang, H.C., 2021. Determining and forecasting drought susceptibility in southwestern Iran using multi-criteria decision-making (MCDM) coupled with CA-Markov model. Sci. Total Environ. 781, 146703.

Peng, K., Jiang, W., Ling, Z., Hou, P., Deng, Y., 2021. Evaluating the potential impacts of land use changes on ecosystem service value under multiple scenarios in support of SDG reporting: A case study of the Wuhan urban agglomeration. Journal of Cleaner Production 307, 127321.

Pontius, R.G., Walker, R., Yao-Kumah, R., Arima, E., Aldrich, S., Caldas, M., Vergara, D., 2007. Accuracy assessment for a simulation model of Amazonian deforestation. Annals Association of American Geographers 97, 677–695.

Pueffel, C., Haase, D., Priess, J.A., 2018. Mapping ecosystem services on brownfields in Leipzig, Germany. Ecosystem Services 30, 73–85.

Qin, X.C., Fu, B.H., 2020. Assessing and predicting changes of the ecosystem service values based on land use/land cover changes with a random forest-cellular automata model in Qingdao metropolitan region, China. Ieee Journal of Selected Topics in Applied Earth Observations and Remote Sensing 13, 6484–6494.

Rasmussen, L.V., Rasmussen, K., Reenberg, A., Proud, S., 2012. A system dynamics approach to land use changes in agro-pastoral systems on the desert margins of Sahel. Agricultural Systems 107, 56–64.

Schirpke, U., Tscholl, S., Tasser, E., 2020. Spatio-temporal changes in ecosystem service values: Effects of land-use changes from past to future (1860–2100). J. Environ. Manage. 272, 111068.

Shao, Y.J., Yuan, X.F., Ma, C.Q., Ma, R.F., Ren, Z.X., 2020. Quantifying the Spatial Association between Land Use Change and Ecosystem Services Value: A Case Study in Xi'an. China. Sustainability 12, 4449.

Song, W., Deng, X., 2017. Land-use/land-cover change and ecosystem service provision in China. Sci. Total Environ. 576, 705–719.

Sun, F., Wang, Y., Chen, Y.N., Li, Y.P., Zhang, Q.F., Qin, J.X., Kayumba, P.M., 2021. Historic and Simulated Desert-Oasis Ecotone Changes in the Arid Tarim River Basin. China. Remote Sensing 13, 647.

van Delden, H., Stuczynski, T., Ciaian, P., Paracchini, M.L., Hurkens, J., Lopatka, A., Shi, Y.E., Prieto, O.G., Calvo, S., van Vliet, J., Vanhout, R., 2010. Integrated assessment of agricultural policies with dynamic land use change modelling. Ecol. Model. 221, 2153–2166.

Verburg, P.H., Overmars, K.P., 2009. Combining top-down and bottom-up dynamics in land use modeling: exploring the future of abandoned farmlands in Europe with the Dyna-CLUE model. Landscape Ecol. 24, 1167–1181.

Wang, Y., Li, X., Zhang, Q., Li, J., Zhou, X., 2018. Projections of future land use changes: Multiple scenarios -based impacts analysis on ecosystem services for Wuhan city. China. Ecol. Indicators 94, 430–445.

Wang, Z., Li, X., Mao, Y., Li, L., Wang, X., Lin, Q., 2022b. Dynamic simulation of land use change and assessment of carbon storage based on climate change scenarios at the city level: A case study of Bortala. China. Ecol. Indicators 134, 108499.

Wang, Q., Wang, H.J., Chang, R.H., Zeng, H.R., Bai, X.P., 2022a. Dynamic simulation patterns and spatiotemporal analysis of land-use/land-cover changes in the Wuhan metropolitan area. China. Ecol. Model. 464, 109850.

Wu, C.Y., Chen, B.W., Huang, X.J., Wei, Y.H.D., 2020. Effect of land-use change and optimization on the ecosystem service values of Jiangsu province. China. Ecol. Indicators 117, 106507.

Wu, J.Y., Luo, J.A., Zhang, H., Qin, S., Yu, M.J., 2022. Projections of land use change and habitat quality assessment by coupling climate change and development patterns. Sci. Total Environ. 847, 157491.

Xie, G.D., Zhang, C.X., Zhen, L., Zhang, L.M., 2017. Dynamic changes in the value of China's ecosystem services. Ecosystem Services 26, 146–154.

Xing, L., Zhu, Y.M., Wang, J.P., 2021. Spatial spillover effects of urbanization on ecosystem services value in Chinese cities. Ecol. Indicators 121, 107028.

Zhang, P., He, L., Fan, X., Huo, P.S., Liu, Y.H., Zhang, T., Pan, Y., Yu, Z.R., 2015. Ecosystem service value assessment and contribution factor analysis of land use change in Miyun County, China. Sustainability 7, 7333–7356.

Zhang, P., Wang, N., Yang, L.W., Zhang, X., Liu, Q., 2020. Evaluation and sensitivity analysis of the ecosystem service functions of haze absorption by green space based on its quality in China. Nature Conservation-Bulgaria 70, 93–141.

Zhang, P., Ma, W.J., Wen, F., Liu, L., Yang, L.W., Song, J., Wang, N., Liu, Q., 2021. Estimating PM2.5 concentration using the machine learning GA-SVM method to improve the land use regression model in Shaanxi, China. Ecotoxicol. Environ. Saf. 225, 112772.

Zhang, S., Yang, P., Xia, J., Wang, W., Cai, W., Chen, N., Hu, S., Luo, X., Li, J., Zhan, C., 2022. Land use/land cover prediction and analysis of the middle reaches of the Yangtze River under different scenarios. Sci. Total Environ. 833, 155238.

Zhang, F., Yushanjiang, A., Jing, Y.Q., 2019. Assessing and predicting changes of the ecosystem service values based on land use/cover change in Ebinur Lake Wetland National Nature Reserve, Xinjiang. China. Sci. Total Environ. 656, 1133–1144.

Zhao, M.M., He, Z.B., Du, J., Chen, L.F., Lin, P.F., Fang, S., 2019. Assessing the effects of ecological engineering on carbon storage by linking the CA-Markov and InVEST models. Ecol. Indicators 98, 29–38.

Zhao, B.X., Li, S.J., Liu, Z.S., 2022. Multi-Scenario Simulation and Prediction of Regional Habitat Quality Based on a System Dynamic and Patch-Generating Land-Use Simulation Coupling Model-A Case Study of Jilin Province. Sustainability 14, 5303.

Zheng, X.Q., Zhao, L., Xiang, W.N., Li, N., Lv, L.N., Yang, X., 2012. A coupled model for simulating spatio-temporal dynamics of land-use change: A case study in Changqing, Jinan. China. Landscape Urban Plann. 106, 51–61.

Zhou, S., Peng, L., 2022. Integrating a mixed-cell cellular automata model and Bayesian belief network for ecosystem services optimization to guide ecological restoration and conservation. LDD 1, 4218.